ELSEVIER

Contents lists available at ScienceDirect

Optics Communications

journal homepage: www.elsevier.com/locate/optcom



Volumetric reconstruction of Brownian motion of a micrometer-size bead in water



Yoon-Sung Bae ^a, Jong-In Song ^a, Dug Young Kim ^{b,*}

- ^a Department of Information and Communications, Gwangju Institute of Science and Technology, Buk-gu, Gwangju 500-712, Republic of Korea
- ^b Department of Physics, Yonsei University, 134 Sinchon-dong, Seodaemun-gu, Seoul 120-749, Republic of Korea

ARTICLE INFO

Article history:
Received 5 June 2013
Received in revised form
10 July 2013
Accepted 26 July 2013
Available online 9 August 2013

Keywords: Digital holography Particle tracking Interference microscopy

ABSTRACT

An effective volumetric measurement and reconstruction scheme for imaging three-dimensional phase objects based on off-axis digital holography is presented. We have experimentally demonstrated the feasibility of our method by observing the Brownian motion of a 3 µm diameter polystyrene bead in water. From a single off-axis hologram of a diffracted field by a sample, a series of transverse intensity images for various axial positions were numerically generated. The center position of the bead sample was pinpointed with a nanometer-scale resolution in 3D space and updated with a frame rate of 30 frames/s. Detailed procedures for elimination of virtual images in an off-axis hologram, reduction of background DC noise, and extraction of exact electric fields in an off-axis hologram are described as advantages of our proposed method over conventional in-line holographic 3D measurement schemes.

© 2013 Elsevier B.V. All rights reserved.

1. Introduction

A holographic image can record the phase as well as the amplitude of an optical field. Since the phase of an optical wave passing through a transparent object can be converted into the thickness or volume of the object with the known refractive index of the material, many experiments have demonstrated the use of digital holographic microscopy (DHM) for thickness or volume measurements of various cells [1-3]. Similar interferometric measurement schemes to obtain the phase of an optical wave through a sample have also been reported as quantitative phase microscopy [4,5]. Another important application of DHM is the imaging and recognition of a three-dimensional (3D) object. Depth information can be retrieved from a holographic image, which contains converging or diverging light fields that are scattered or diffracted from an object. Once a complex optical field is obtained with DHM on a given two-dimensional (2D) transverse plane along the propagation direction of light, 2D optical fields on the other axial positions can be numerically calculated [6-10]. This numerical focusing based on a diffraction theory enables us to reconstruct 3D optical fields originating from a sample.

Numerical signal processing in DHM can be used to correct image aberrations [11,12], to improve the resolution of an imaging system [8,10], or to reconstruct the 3D volumetric structures of an object with various computational methods [13–15]. Lately, these

digital signal processing techniques have been applied to digital in-line holography for 3D tracking of nanometer size particles [16,17]. Since 3D volumetric image reconstruction or 3D structural recognition of an object can be obtained from a single measured hologram, high-speed 3D tracking of a nanometer size particle becomes possible with these digital holographic imaging and signal processing techniques. Even though in-line DHM has great advantages such as a superb axial resolution and wide axial tracking range, it has intrinsic limitations such as the ambiguity of a twin-image or overlapping noise from undiffracted zero-order light in numerical image reconstruction [8,18-20]. Therefore, the exact reconstruction of an optical field from an in-line hologram is often difficult, and the 3D information of an object is obtained by comparing a stack of numerically generated transverse intensity images with either a series of premeasured depth dependent intensity patterns [10,21,22] or a series of calculated intensity patterns from the analytic Mie scattering formula [16,23].

In order to circumvent these undesired problems of in-line holographic 3D particle tracking methods, we present a method based on off-axis DHM in this paper. This study demonstrates a 3D imaging and tracking scheme for a micrometer-size polystyrene bead using off-axis DHM by tracing the focused spot of transmitted light with a micrometer-sized spherical dielectric sample that works as a small ball lens. Unlike previous approaches, our method can eliminate problems associated with virtual images and background DC noises in a hologram. Since the exact interfered electric field can be obtained from an off-axis hologram, numerical focusing with a diffraction formula can be used in our method. This is an another important advantage of particle

^{*}Corresponding author. Tel.: +82 221235611.

E-mail address: dykim1@yonsei.ac.kr (D.Y. Kim).

tracking with off-axis holography, which produces much better spatial resolution in our method compared to conventional particle tracking methods based on in-line holography. The 3D position of the sample was obtained by finding the focused spot of light from the sample, which was calculated from a measured off-focus hologram. By fitting the depth-dependent intensities of the transverse images at the peak position as a function of the propagation distance with a paraxial curve, we were able to locate the 3D position of the sample bead within nanometer range accuracy. The fast Brownian motion of a 3 μm diameter polystyrene bead in water was observed with our proposed method, and the feasibility of this method was demonstrated by measuring the mean square distance (MSD) of a particle in Brownian motion.

2. Experimental setup

We constructed a transmission digital holographic microscope with an off-axis configuration based on a Mach-Zehnder interferometer. A linearly polarized HeNe laser (JDSU 1137P) with an output power of 7 mW with a 632.8 nm wavelength was used as a coherent light source. The laser light is split into the reference and object beams by beam splitter BS1 to form a Mach-Zehnder interferometer. Collimated light in the sample arm illuminates a sample, and the transmitted light through the sample is magnified by an oil immersion objective lens with a 1.3 numerical aperture (NA) (Olympus UPlanFL N). We used a $60 \times$ objective lens for L2 to expand the reference beam of the interferometer. An interfered image of the two lights is formed with the non-polarizing beam splitter and is acquired by a CMOS image sensor (Mikrotron MC1362), on which 640 × 480 pixels are used for image acquisition. The size of each pixel is 14 square um, and the measured optical intensities are digitized into 10-bit binary data. Fig. 2 shows a measured off-axis hologram for a polystyrene bead in water. Large circular fringes from the sample bead are overlapped with tiny diagonal fringes. The tilting angle and period of the diagonal fringes are set by adjusting the angle between the reference and object beam in the experiment.

3. Position tracking algorithm

In order to obtain the numerical reconstruction of diffracted light near a sample from a measured hologram, we used a $3 \mu m$ diameter polystyrene bead with a refractive index of 1.587 at a 632.8 nm wavelength. A measured hologram by the detector array in Fig. 1 is the interfered intensity image between an object beam and a reference beam and can be described as [6,7]

$$h(x,y) = |r(x,y)|^2 + |o(x,y)|^2 + r(x,y)o^*(x,y) + r^*(x,y)o(x,y)$$
(1)

where r(x,y) and o(x,y) are the complex optical fields corresponding

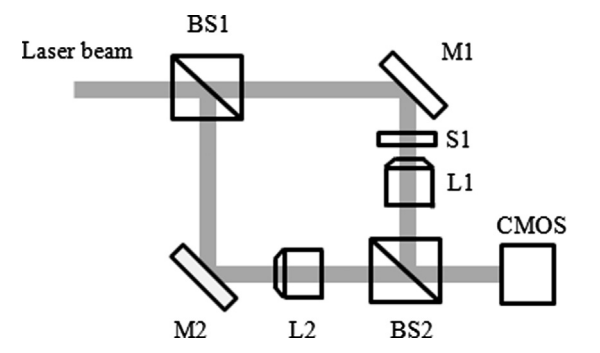


Fig. 1. Experiment setup. BS1 and BS2: 1st and 2nd beam splitters; L1 and L2: objective lenses; S: sample holder; M1 and M2: mirrors; CMOS: array detector.

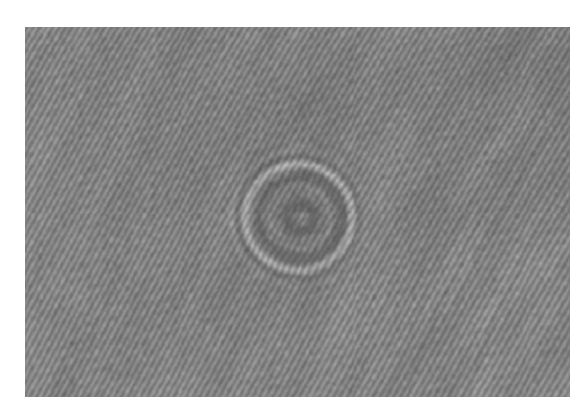


Fig. 2. Measured off-axis hologram of a 3 μm polystyrene bead in water.

to the reference and object lights, respectively. * represents the complex conjugate. We expanded the reference beam with the objective lens L2 in Fig. 1 to form a diverging reference beam with a large radius of curvature on the detector. This helps to make the fringe spacing of the diagonal fringes shown in Fig. 1 to be uniform. Since both the object and the reference beams are diverging, we can rewrite the reference and the object lights with [12]

$$\begin{cases} r(x,y) = A \exp[i2\pi(f_{x0}x + f_{y0}y)] \exp[iW_R(x,y)] \\ o(x,y) = B \exp[i\pi(x,y)] \exp[iW_O(x,y)] \end{cases}, \tag{2}$$

where A, B are constants, and f_{x0} and f_{y0} are fixed frequencies along the x and y axes. f_{x0} and f_{y0} can be adjusted by tilting the beam splitter BS2 or the mirror M2 in Fig. 1. $W_0(x,y)$ and $W_R(x,y)$ are diverging phases introduced by the two objective lens L1 and L2, and $\phi(x,y)$ is the phase function of the sample detected by the CMOS chip shown in Fig. 1. Then, the last term in Eq. (1) can be rewritten as

$$I_{h}^{F}(x,y) \equiv r^{*}(x,y)o(x,y) = A^{*}B \exp\left[-i2\pi(f_{x0}x + f_{y0}y)\right]$$
$$\exp[i(\phi(x,y) + W_{O}(x,y) - iW_{R}(x,y))]$$
(3)

This is a filtered hologram of h(x,y) given in Eq.(1). When $H(f_x,f_y)$ is the Fourier transformed function of h(x,y), Fig. 3 shows the intensity distribution of the Fourier transformed function $|H(f_x,f_y)|$ in the frequency-domain calculated from the hologram shown in Fig.2. The Fourier transformed function corresponding to the first and the second terms in Eq. (1) are distributed around the origin, while the third and the forth terms are centered at (f_{x0}, f_{y0}) and $(-f_{x0}, -f_{y0})$, respectively.

We obtain $I_h^F(x,y)$ by taking only the 3rd quadrant of $H(f_x f_y)$ and the subsequent inverse Fourier transform of it. Unlike most of previously reported papers where magnified field on the object side of an imaging system was used to obtain diffracted fields near an object, we have used measured field $\exp[i\phi(x,y)]$ itself to calculate off-focused fields on the image side of a system.

Fig. 4 shows the schematic diagram of our tracking method. S_{02} is the distance between the objective lens (L1) and the detector plane on the image side of Fig. 4, while S_{01} is the distance between the lens and the corresponding conjugate object plane on the object side of the imaging system. S_{01} and S_{02} are related with the thin lens equation; $1/f = 1/S_{01} + 1/S_{02}$. We consider a sample located d_{m1} distance apart from the object plane toward the direction of the lens. When the distance from the objective lens to the sample is S_{m1} , and the distance from the lens to its corresponding image is S_{m2} , we have another the thin lens equation satisfying $1/f = 1/S_{m1} + 1/S_{m2}$. If the diverging phase in the object field $\exp[iW_O(x,y)]$ is not removed, we would obtain a focused image at d_{m2} distance apart on the right side of the detector plane with numerical focusing. We have removed the diverging phase of $\exp[i(W_O(x,y)-W_R(x,y))]$ in measured

Download English Version:

https://daneshyari.com/en/article/7932389

Download Persian Version:

https://daneshyari.com/article/7932389

Daneshyari.com